Published in final edited form as:
Dev Biol. 2008 August 1; 320(1): 122–130. doi:10.1016/j.ydbio.2008.04.043.

Modulation of ionizing radiation-induced apoptosis by *bantam* microRNA in *Drosophila*

Burnley Jaklevic[1], **Lyle Uyetake**, **Anita Wichmann**, **Amber Bilak**, **Christopher English**, and **Tin Tin Su**[2]

Department of Molecular Cellular and Developmental Biology, University of Colorado, Boulder, CO 80309-0347, USA

Abstract

In *Drosophila*, heterozygocity in the pro-apoptotic gene *hid* significantly reduces apoptosis that is induced by ionizing radiation (IR). Therefore, mechanisms that regulate Hid levels can potentially contribute to life-or-death decision of an irradiated cell. 3'UTR of *hid* mRNA contains 5 potential binding sites for *bantam* microRNA. Ectopic expression of *ban* attnuated apoptosis that results from ectopic expression of *hid* but the significance of this regulation under physiological conditions remained to be investigated. We report here that *ban* is needed to limit IR-induced apoptosis in larval imaginal discs. Using tubulin-EGFP *ban* sensors with *ban* consensus sequences in the 3'UTR, we find that EGFP decreases following IR, indicating that IR activates *ban*. Likewise, a tubulin-EGFP reporter with *hid*-3'UTR is repressed in irradiated discs and this repression requires *ban* consensus sites in the *hid* 3'UTR. *ban* mutant larvae show increased sensitivity to killing by IR, which is suppressed by a mutation in *hid*. These results can fit into a model in which IR activates *ban* and *ban* represses *hid* to limit IR-induced apoptosis. miRNAs have been shown previously to be induced by radiation but this is the first report that a miRNA is functionally important for radiation responses.

Keywords

Drosophila; radiation; apoptosis; microRNA; bantam; hid

Introduction

The role of non-protein coding RNAs in gene expression is well established (e.g. ribosomal RNAs). More recent work demonstrates the role of small (~20nt) microRNAs (miRNA) in gene regulation (Alvarez-Garcia and Miska, 2005; Bartel, 2004; Tang, 2005). They are thought to bind and render the target mRNA unstable when the binding site is a perfect match or to interfere with translation when there is mismatch within the binding site (Tang, 2005). miRNAs act in diverse processes including the timing of developmental transitions in *C. elegans*, hematopoiesis and carcinogenesis in mammals, and cell cycle regulation and cell death in *Drosophila* (Alvarez-Garcia and Miska, 2005; Bartel, 2004; Boehm and Slack, 2005; Brennecke et al., 2003; He et al., 2005; Johnson et al., 2005).

2Corresponding author: Tin.su@colorado.edu, 303-735-3245 (Phone), 303-492-7744 (Fax).
1Present address: Department of Molecular and Cell Biology and Helen Wills Neuroscience Institute, 291 Life Sciences Addition, University of California, Berkeley, Berkeley, California 94720, USA.

Drosophila bantam was identified in a screen for genes that, when overexpressed, produced excessive tissue growth (Hipfner et al., 2002). *ban* encodes a 21 nt miRNA that is required for proper growth of larval imaginal discs (Brennecke et al., 2003). Imaginal discs are organ precursors that are set aside during embryogenesis. During the three larval stages (also called 'instars'), imaginal discs enlarge by mitotic proliferation. During metamorphosis in the pupae, imaginal discs differentiate into respective adult structures (eye imaginal discs into eyes and wing imaginal discs into wings, etc.). Under-proliferation or excessive cell death in imaginal discs can lead to reduction of adult structures, and can result in reduction of adult viability. Therefore, survival of imaginal discs, after exposure to genotoxins such as ionization radiation or (IR), can be scored as the ability of larvae to develop into viable adults that eclose from the pupal case.

Loss of function mutations in *ban* reduced the growth of larval imaginal discs. Ectopic induction of *ban* had the opposite effect, promoting cell proliferation, inhibiting apoptosis, and causing overgrowth of imaginal discs (Brennecke et al., 2003). Targets of *ban* in cell proliferation remains unknown but bioinformatics searches identified 5 potential *ban* sites in the 3'UTR of the pro-apoptotic gene *hid*. A transgene reporter that consists of tubulin promoter driven EGFP coding sequences fused to *hid* 3'UTR responds to *ban*; overexpression of *ban* reduced the EGFP signal. EGFP was reduced but to a lesser degree when the two most conserved *ban* target sites were deleted (Brennecke et al., 2003). Ectopic *ban* can also suppress experimentally induced apoptosis caused by over-expression of *hid*. Thus *hid* appears to be a *bona fide* target of post-transcriptional regulation by *ban*. The significance of this regulation under physiological conditions (i.e. not in ectopic expression studies) has not been addressed.

Apoptosis is a key cellular response to DNA double strand breaks (DSBs) such as those induced by IR. In metazoa including *Drosophila*, homologs of the tumor suppressor p53 becomes activated in response to DNA damage and induces apoptosis (Brodsky et al., 2000; Brodsky et al., 2004; Jin et al., 2000; Lee et al., 2003; Lowe et al., 1993; Ollmann et al., 2000; Peters et al., 2002; Sogame et al., 2003; Takai et al., 2002). Apoptosis requires the activity of caspases, which are normally rendered inactive by being bound to IAPs (*i*nhibitor of apoptosis *p*roteins). p53-mediated transcription overcomes this inhibition by leading to increased levels or activity of Smac /DIABLO orthologs (Hid, Rpr, Grim and Skl in *Drosophila*) (Brodsky et al., 2000; Brodsky et al., 2004; Kornbluth and White, 2005; Wichmann et al., 2006). Smac /DIABLO then binds to IAPs and frees up caspases (Schuler and Green, 2001).

Pro-apoptotic genes such as *hid* and *rpr* are essential for fly development and viability because they are essential for developmental programmed cell death (eg. (Grether et al., 1995)). *Drosophila* p53, however, is dispensable for development, viability and developmental cell death, indicating that other regulators act on pro-apoptotic genes in a developmental context. This leads to the question of which context *ban* microRNA functions in to regulate *hid*. In other words, *ban* may be an important regulator of *hid* but whether this regulation is important for developmental cell death, damage-induced cell death or both, remains to be determined.

To investigate the role of *ban* in responses to damage caused by IR, we analyzed cell and organismal death in *ban* mutants following irradiation. Here, we present data that suggest a role for *ban* in cellular and organismal responses to IR and identify *hid* as an important mediator of *ban*-dependent responses. Expression of microRNAs has been shown to be induced by radiation in murine and plant cells (Ishii and Saito, 2006; Zhou et al., 2007), but this is the first report of the functional importance of a microRNA in radiation responses in any system.

Results

We first present three lines of data that support the idea that *ban* coordinates cellular and organismal responses to ionizing radiation. These are (1) *ban* mutants suffer more IR-induced apoptosis, (2) *ban* is activated by IR, and (3) *ban* mutant larvae are more sensitive to killing by IR.

(1) ban mutants suffer more IR-induced apoptosis

Larvae homozygous for null alleles of *ban* show poor growth of imaginal discs and die as pupae (Brennecke et al., 2003; Hipfner et al., 2002). Imaginal discs from one such mutant, $ban^{\Delta 1}$ that results from a deletion of the *ban* locus, stain strongly with Acridine Orange (Fig. 1). AO stains apoptotic cells specifically in *Drosophila* (Abrams et al., 1993), suggesting that loss of *ban* leads to spontaneous apoptosis. Homozygotes of a strong hypomorphic allele, $ban^{EP(3)3622}$, or hemizygotes of the same over $ban^{\Delta 1}$ survive to adulthood (Brennecke et al., 2003; Hipfner et al., 2002). *ban* mutants of these allelic combinations show wild type level of apoptosis (Fig. 1A), allowing us to determine if *ban* also has a role in apoptosis induced by IR. Exposure to 400R of X-rays produces a small increase in AO stain in discs from wild type larvae (Fig. 1A and quantified in B). Under identical conditions, imaginal discs in $ban^{EP(3)3622}$ homo- or hemizygotes show significantly higher levels of AO staining than wild type. We conclude that *ban* mutants undergo IR-induced apoptosis more readily than wild type. These results suggest that *ban* is required to limit both spontaneous and IR-induced apoptosis. In subsequent experiments, we focus on the role of *ban* in IR-induced apoptosis.

The increase in AO staining after irradiation is higher for ban^{EP3362} homozygotes than for ban^{EP3362}/ $ban^{\Delta 1}$ hemizygotes (Fig. 1). ban^{EP3362} homozygotes are also less viable than ban^{EP3362}/ $ban^{\Delta 1}$ hemizygotes, with and without irradiation (Fig. 3 and below). We do not know why the phenotypes of ban^{EP3362} homozygotes are more severe than those of ban^{EP3362}/ $ban^{\Delta 1}$ hemizygotes, but speculate that the inserted P-element may be affecting more than one gene, which is a common occurrence in *Drosophila*.

(2) EGFP bantam sensor shows activation of ban by IR

A transgene reporter consisting of tubulin promoter-driven EGFP with two copies of a perfect *ban* target sequence in the 3'UTR (called '*bantam* sensor') can distinguish as little as 2-fold changes in *ban* levels (Brennecke et al., 2003). We find that exposure to X-rays results in a decrease in *bantam* sensor fluorescence in the imaginal discs and brains of irradiated 3rd instar larvae (Fig. 2A–L, quantified for wing discs in M). A decrease in EGFP signal reflects an increase in the activity of its repressor, *ban*. Little or no change in EGFP was seen at 5 and 18 hr after irradiation. The first time at which a significant decrease in EGFP could be observed was at 24 hr after irradiation. The half-life of EGFP is approximately 24hr. Therefore, we infer that the increase in *ban* activity occurred soon after irradiation to show a visible difference at 24 hr after irradiation. The difference in EGFP signal between irradiated and un-irradiated larvae was confirmed by Western blotting of the 24 hr samples (Fig. 2N). This time point was analyzed because it is the earliest after irradiation that we see a significant decrease in EGFP signal (Fig.2 I, J and M). It is unlikely that the difference in EGFP expression is due to a general decrease in macromolecular synthesis after irradiation; we do not see a change in the level of β-tubulin (Fig. 2N) or EGFP from a control transgene rendered unresponsive to *ban* (Fig. 6G).

(3) ban mutants are radiation sensitive

To examine the importance of *ban* at the organismal level, we assayed for survival of *ban* mutant larvae after exposure to 0–4000R of X-rays. This dose is typically used in viability studies because most larvae eclose into adults but approximately half of the adults die soon thereafter (Jaklevic and Su, 2004). Therefore, we are causing significant damage and yet are

allowing a significant fraction of animals to survive. Thus we hope to understand mechanisms that kill larvae as well as those that allow survival. Under these conditions, *ban* mutants show decreased survival to adulthood after irradiation (Fig. 3). This effect is seen for both allelic combinations of *ban* (Fig. 3A) and also for *ban* heterozygotes (Fig. 3B). We conclude that *ban* is required to ensure survival at both the cellular and the organismal levels after exposure to IR.

Collectively, the three lines of evidence described above implicate *ban* in cellular and organismal responses to IR. More specifically, experiments with *ban* sensor indicate a change in *ban* activity shortly after irradiation.

Changes in ban sensor are dependent on p53

To address the link between IR and *ban* activity, we examined the role of p53, which mediates many IR responses. Under normal growth conditions, there are no obvious deviations from wild type in *ban* sensor expression in p53 mutants, which are homozygous viable and show little or no defects (Fig. 4A). Therefore, it is unlikely that p53 has a role in regulation of *ban* activity normally. p53 mutants also show a increase in *ban* sensor fluorescence with larval development (Fig. S1) indicating that the sensor can respond to changes in *ban* levels, which normally occurs during development (Brennecke et al., 2003), in the absence of p53.

Following irradiation, we found that *ban* sensor expression no longer changed in the wing imginal discs of p53 mutant larvae (Fig. 4B and quantified in C). The lack of change was confirmed by Western blotting for EGFP (Fig. 4D). These data suggest that p53 is required for the IR-induced decrease in *ban* sensor expression, which reflects an increase in *ban* activity.

Since p53 is a transcriptional activator, we addressed the possibility that p53-dependent activation of *ban* after irradiation occurs via an increase in *ban* levels. Northern blots of extracts from larval brains and imaginal discs show a band at the predicted size for mature *ban* miRNA (~20 nt), which is absent in *ban* mutants (Fig. 5). After irradiation, however, there was no detectable change in *ban* levels in whole larvae (Fig. 5A, quantified in B). Similar results were obtained using extracts of imaginal discs and brains also at 6–24 hr after irradiation, and in both wild type and p53 mutant larvae (Fig. 5B and D, and data not shown). While we cannot rule out that there may be regional changes in *ban* levels within the tissues, we conclude that bulk *ban* levels do not change significantly after irradiation despite a change in *ban* activity.

The data from Northern blots help us rule out an alternate explanation for the change in *ban* sensor fluorescence, that development arrests at the time of irradiation, while it progresses for 24 hr in unirradiated discs. Because *ban* levels declines normally with larval development, this could result in a difference in EGFP signals documented in Fig. 2. Northern blots show, however, that *ban* level is similar regardless of irradiation for up to 24 hr, suggesting that development has progressed normally in irradiated and control larvae, at least as far as *ban* expression is concerned. Northern blots shown have been optimized for comparing irradiated and control samples at each time point, and not for visualizing the developmental decline in *ban* levels.

Cell death is required for optimal changes in ban sensor after irradiation

p53 mutants display reduced and delayed apoptosis compared to wild type after irradiation (Wichmann et al., 2006). This suggests the possibility that the requirement for p53 in *ban* activation reflects simply a requirement for p53 in timely and optimal induction of apoptosis. In other words, induction of apoptosis may be required to activate *ban*; p53 mutants fail to activate *ban* because they are defective for induction of apoptosis. To ask if apoptosis is required for *ban* activation, we blocked radiation induced apoptosis using p35, a viral caspase

inhibitor. p35 was expressed in the posterior half of wing imaginal discs using the hh-GAL4>UAS system so that the anterior half could serve as a control. As expected, exposure to 4000R of X-rays produced robust apoptosis in anterior half of wing discs but not in the posterior half (Fig. 6D). We find that *ban* sensor levels decreased as expected in the control anterior half of each irradiated disc where cell death was robust (Fig. 6C). A similar decrease was not observed in the posterior half. We conclude that cell death is required for optimal activation of *ban* after irradiation. We infer from these results that the role of p53 in *ban* activation could be explained by the role of p53 in proper induction of apoptosis. We cannot, however, rule out other modes of contribution by p53.

Hid is an important ban target in IR responses

Previous experiments identified *hid* as a target of *ban*, though not under irradiation conditions. Therefore, we examined the possibility that *hid* is a target of *ban* after irradiation as well. A transgene reporter that consists of tubulin promoter driven EGFP coding sequences fused to the *hid* 3'UTR responds to *ban* (called '*hid-UTR* sensor'); overexpression of *ban* reduced the EGFP signal and this reduction was less pronounced when the two most conserved *ban* target sites were deleted (Brennecke et al., 2003). This is consistent with the known role of miRNAs in regulation of gene expression: binding of miRNAs to the 3'UTR of target mRNAs reduces the stability or the translation efficiency of the latter (Tang, 2005). We find that EGFP signal from the *hid-UTR* sensor was lower in imaginal discs from irradiated larvae, compared to unirradiated controls (Fig. 7 A and C, quantified as 'hid' in E), although this decrease was smaller than the decrease for *ban* sensor that contains perfect sequence matches to *ban* (Fig. 2M). The decrease in EGFP signal was seen when the *hid-UTR* sensor contained all 5 putative *ban* target sequences but not when the two most conserved sites had been deleted (Fig. 7, compare D to B, quantified as 'hid Δ1,4' in E). Changes in EGFP fluorescence were confirmed by Western blotting. The difference in EGFP from the *hid-UTR* sensor was visible by 24 hr after irradiation with 4000 R (Fig. 7) but not at earlier times (not shown). The half-life of EGFP (~24hr) likely contributes to this delay and suggests that changes in regulation of gene expression via the *hid3'UTR* occurred soon after irradiation. Moreover, the lack of change in EGFP from the mutant *hid-UTR* sensor suggests that this regulation is mediated by *ban* binding sites.

We monitored the level of EGFP mRNA and find no significant changes in levels after irradiation. These results support the idea that regulation by *ban* via *hid* 3'UTR occurs post-transcriptionally.

Reduction of hid gene dosage rescues radiation sensitivity of ban mutants

If repression of Hid by *ban* is important for survival of irradiated larvae, we expect that reduction of *hid* by mutation would rescue lethality of irradiated *ban* mutants. This appears to be the case. *ban, hid* double heterozygotes survived irradiation better than did *ban* heterozygotes and this difference was statistically significant at 4000R ($p=0.003$) (Fig. 3B). In fact, *hid* heterozygocity restored the survival of *ban hid*/TM6 heterozygotes to that of TM6 balancer heterozygotes. H99 deficiency deletes the *hid* gene and serves as a control.

Discussion

The pro-apoptotic gene *hid* gene is haplo-insufficient for IR-induced apoptosis; reduction of *hid* gene dosage by half reduced IR-induced apoptosis to control levels (Brodsky et al., 2004). This effect is specific to IR-induced apoptosis because reduction of *hid* gene dosage by half did not affect developmental cell death and allowed the survival of flies heterozygous for the chromosomal deficiency H99 that deletes *hid, rpr* and *grim*. Thus mechanisms that change

hid levels by as little as 2-fold can potentially affect the life-or-death decisions of a cell with DNA double strand breaks. Our results suggest that *ban* may provide one such activity.

Three lines of data implicate *ban* in responses to IR: exposure to X-rays results in increased *ban* activity in larval imaginal discs, *ban* confers survival to irradiated cells (i.e. helps limit apoptosis) and *ban* confers survival to irradiated larvae.

Previous work has shown that *hid* is a downstream target of p53. In *Drosophila* embryos, IR results in an increase in *hid* mRNA and this increase is not seen in p53 mutants (Brodsky et al., 2004). In larvae, IR also results in an increase in *hid* mRNA and this increase is delayed by 16 hr in p53 mutants (Wichmann et al., 2006). How p53 targets *hid* is not known and, unlike in the case of *rpr*, there is no evidence that *hid* is a direct transcriptional target of p53. We find that although *ban* activation is dependent on p53, this is likely an indirect effect because *ban* levels remain unchanged. We also find that apoptosis is required for activation of *ban*, which can explain the dependence on p53. These results may fit into a model in which exposure to IR results in transcriptional induction of *hid*, and apoptosis. Apoptosis activates ban by an unknown mechanism. *ban* represses *hid* post-transcriptionally and limits apoptosis, allowing for survival of cells and of organisms. The balance between *ban* and *hid* appears to contribute to the life-death decision; reducing *ban* gene dosage by half results in increased killing by IR, but the increase in larval lethality can be rescued by a concurrent reduction in *hid* gene dosage by half.

In our radiation experiments, we induce death in individual cells scattered throughout the imaginal disc, but see changes in *ban* sensor throughout the disc. By blocking apoptosis with p35, we found that apoptosis is required for activation of *ban* after irradiation. These observations are consistent with the idea that apoptotic cells activate *ban*, presumably in the neighbors. There is precedent for such an idea; dying cells in larval imaginal discs have been shown to signal their neighbors to enter S phase (Ryoo et al., 2004) or to proliferate (Wells et al., 2006). If non-cell autonomous induction is activating *ban* in our experiments, it apparently does not operate across the compartment boundary because dead cells in the anterior compartment could not activate *ban* in the posterior compartment (Fig. 6).

After finding that apoptosis was necessary to activate *ban*, we made attempts to determine if apoptosis is sufficient to activate *ban*. We induced apoptosis in a subset of imaginal disc cells by ectopic expression of *hid*, *rpr* or Diptheria Toxin using several different GAL4-UAS systems. We saw no change in *ban* sensor levels in these experiments (not shown), but cell death induced by these protocols was less robust than cell death induced by our radiation protocols, making the results inconclusive. We were able to induce robust cell death by heat-shock induction of Hid, but this treatment resulted in larval death within 10 hr, precluding analysis of *ban* sensor 24 hr after induction of cell death.

The finding that *ban* activity increased after irradiation while *ban* levels remained unchanged was a surprise. The current view is that changes in miRNA activity results directly from changes in miRNA levels. Our observations provide the first indication that regulation of miRNA activity may be more complex and can occur without a change in miRNA levels. Further work is required to determine if such regulation occurs for other miRNAs and in other systems and what molecular mechanisms are responsible. We are currently performing a genetic screen for modifiers of IR sensitivity in *ban* mutants. Such a screen may yield upstream regulators that activate *ban* after irradiation.

Published data link p53 to *ban* through the Hippo tumor suppressor pathway. First, under normal (non-irradiation) conditions, *ban* transcription is activated by Yorkie, a transcriptional co-activator that is negatively regulated by Hpo (Nolo et al., 2006; Thompson and Cohen, 2006). After irradiation, Hpo is activated by p53 (Colombani et al., 2006). If these regulatory

relationships were conserved regardless of conditions (irradiated versus normal), a combination of results from these studies would lead one to expect p53 to *repress ban* expression, both during normal growth and following irradiation. Instead, we find little change in *ban* levels after irradiation. In other words, p53-dependent activation of Hippo after irradiation appears to have little effect on *ban* levels. These considerations lead us to conclude that regulatory circuits operate differently between normal growth conditions and following irradiation.

Of all the possible cellular responses to DNA DSBs, how one response is chosen over another, cell cycle arrest and DNA repair vs. apoptosis, for example, remains unclear. Mammalian p53 is activated by IR and induces gene products needed for DNA repair, cell cycle arrest and apoptosis. Activation of p53 alone, therefore, cannot account for the choice of cellular responses. Rather, it is the additional layer of regulation provided by regulators that differentially modulate various p53 targets that directs an irradiated cell into living or dying. *Drosophila* p53 contributes to apoptosis and to DNA repair (Brodsky et al., 2004). Therefore, as in the case of mammalian p53, additional inputs may be important in channeling an irradiated cell into one fate but not the other. Molecules such as *ban* can impose an additional level of regulation beyond by antagonizing a target of p53, Hid, thereby profoundly influencing whether a cell or an organism lives or die.

Finally, we note that *ban* is also required to prevent spontaneous apoptosis in the absence of irradiation (Fig. 1). It remains to be determined if *hid* or another pro-apoptotic gene is an important target for *ban* in this process, but it is possible that excess cell death, in addition to reduced proliferation as previously reported, contribute to the previously reported pupal lethality of *ban* null mutants (Brennecke et al., 2003).

Materials and Methods

Fly stocks

All fly stocks used here have been described: $p53^{5A\text{-}1\text{-}4}$ allele is a null generated by site directed partial deletion of the gene (Rong et al., 2002); ban^{EP3362} and $ban^{\Delta 1}$ alleles were caused by a P-element insertion and by imprecise excision of the P-element (Brennecke et al., 2003). Fly stocks with EGFP *ban* sensors have been described (Brennecke et al., 2003). 20.1 is an insertion on III and 20.X is an insertion on II; both are homozygous viable. $Hid^{I(3)05014}$ contains a P-element insertion between amino acids 105 and 106 (Grether et al., 1995). Hedgehog (hh)-GAL4>UAS-p35 expression system has been described before (Wells et al., 2006).

Irradiation and Acridine Orange staining

Larvae were irradiated 96±4 hr after egg deposition (except for Fig. 4C where larvae were 94–110 hr old) in a TORREX X-ray generator set at 5 mA and 115 kV and dissected in PBS. The discs were stained in 100 μM AO in PBS for 5 min, washed twice in PBS, mounted in PBS and imaged using a Leica DMR microscope and Slidebook software (Intelligent Imaging). Exposure time and all subsequent treatments of images are identical between control and experimental samples.

GFP imaging

The discs and CNS were mounted in PBS and imaged using a Leica DMR microscope and Slidebook software (Intelligent Imaging). Exposure time and all subsequent treatments of images are identical between control and experimental samples. For fluorescence quantification, mean fluorescence intensity (total pixel volume above background/total disc area) was read for each wing disc using Slidebook. This value for each disc was normalized by dividing by the maximal intensity value from among un-irradiated discs for a particular

experiment. After normalization, average and standard error of mean (SEM) were calculated for the entire irradiated or unirradiated population.

Western blots

CNS, imaginal discs and salivary glands were dissected and homogenized in PBS and boiled in SDS sample buffer. The samples were separated on 10% SDS PAGE and blotted on PVDF membranes. The membranes were probed with 1:1000–2000 rabbit anti-EGFP antibody (Molecular Probes) and 1:300–1000 anti-β-tubulin antibody (E7; Developmental Hybridoma Bank), followed by HRP-conjugated secondary antibodies and ECL detection.

Northern blots

Larvae were irradiated as described above at 96±4 hr egg deposition. At 1.5 3, 6, 12, 18 or 24 hr after irradiation, whole larvae or imaginal discs and CNS were dissected in PBS and homogenized in cold (4°C) PBS. Total RNA was isolated using a Invitrogen TRIzol kit and separated on TBE-Urea gels according to manufacturer's instructions (Ambion). The samples were blotted onto Hybond N (Amersham) via capillary transfer and crosslinked in a Stratalinker (Stratagene). The blots were probed with a ^{32}P end-labeled anti-*ban* oligonucleotide (ACAAAATCAGCTTTCAAAATGATCTCACTTGT). Unlabelled *ban* DNA oligonucleotide was also loaded as a positive control (not shown). The blots were re-probed with a ^{32}P end-labeled anti-5S ribosomal RNA oligonucleotide (GCGGTCCCCCATCTAAGTACTAACC) to control for equal loading. ^{32}P signals were quantified using a phosphoimager (Molecular Dynamics).

Supplementary Material

Refer to Web version on PubMed Central for supplementary material.

Acknowledgements

We thank the Bloomington Drosophila Stock Center and Michael Brodsky for fly stocks and the Cohen and Johnston labs for fly stocks, protocols and helpful suggestions. We are especially indebted to Julius Brennecke for help with the Northern blots. We thank Patrick O'Farrell, Laura Johnston, Kristin Scott and members of the Su lab for comments and helpful suggestions. We thank Nancy Kim for help with survival experiments. This work was funded by a grant from the National Institute of Health (GM66441) to T. T. S. and an ARCS scholarship to B.J.

References

Abrams JM, White K, Fessler LI, Steller H. Programmed cell death during Drosophila embryogenesis. Development 1993;117:29–43. [PubMed: 8223253]

Alvarez-Garcia I, Miska EA. MicroRNA functions in animal development and human disease. Development 2005;132:4653–4662. [PubMed: 16224045]

Bartel DP. MicroRNAs: genomics, biogenesis, mechanism, and function. Cell 2004;116:281–297. [PubMed: 14744438]

Boehm M, Slack F. A developmental timing microRNA and its target regulate life span in C. elegans. Science 2005;310:1954–1957. [PubMed: 16373574]

Brennecke J, Hipfner DR, Stark A, Russell RB, Cohen SM. bantam encodes a developmentally regulated microRNA that controls cell proliferation and regulates the proapoptotic gene hid in Drosophila. Cell 2003;113:25–36. [PubMed: 12679032]

Brodsky MH, Sekelsky JJ, Tsang G, Hawley RS, Rubin GM. mus304 encodes a novel DNA damage checkpoint protein required during Drosophila development. Genes Dev 2000;14:666–678. [PubMed: 10733527]

Brodsky MH, Weinert BT, Tsang G, Rong YS, McGinnis NM, Golic KG, Rio DC, Rubin GM. Drosophila melanogaster MNK/Chk2 and p53 regulate multiple DNA repair and apoptotic pathways following DNA damage. Mol Cell Biol 2004;24:1219–1231. [PubMed: 14729967]

Colombani J, Polesello C, Josue F, Tapon N. Dmp53 activates the Hippo pathway to promote cell death in response to DNA damage. Curr Biol 2006;16:1453–1458. [PubMed: 16860746]

Grether ME, Abrams JM, Agapite J, White K, Steller H. The head involution defective gene of Drosophila melanogaster functions in programmed cell death. Genes Dev 1995;9:1694–1708. [PubMed: 7622034]

He L, Thomson JM, Hemann MT, Hernando-Monge E, Mu D, Goodson S, Powers S, Cordon-Cardo C, Lowe SW, Hannon GJ, Hammond SM. A microRNA polycistron as a potential human oncogene. Nature 2005;435:828–833. [PubMed: 15944707]

Hipfner DR, Weigmann K, Cohen SM. The bantam gene regulates Drosophila growth. Genetics 2002;161:1527–1537. [PubMed: 12196398]

Ishii H, Saito T. Radiation-induced response of micro RNA expression in murine embryonic stem cells. Med Chem 2006;2:555–563. [PubMed: 17105436]

Jaklevic BR, Su TT. Relative contribution of DNA repair, cell cycle checkpoints, and cell death to survival after DNA damage in Drosophila larvae. Curr Biol 2004;14:23–32. [PubMed: 14711410]

Jin S, Martinek S, Joo WS, Wortman JR, Mirkovic N, Sali A, Yandell MD, Pavletich NP, Young MW, Levine AJ. Identification and characterization of a p53 homologue in Drosophila melanogaster. Proc Natl Acad Sci U S A 2000;97:7301–7306. [PubMed: 10860994]

Johnson SM, Grosshans H, Shingara J, Byrom M, Jarvis R, Cheng A, Labourier E, Reinert KL, Brown D, Slack FJ. RAS is regulated by the let-7 microRNA family. Cell 2005;120:635–647. [PubMed: 15766527]

Kornbluth S, White K. Apoptosis in Drosophila: neither fish nor fowl (nor man, nor worm). J Cell Sci 2005;118:1779–1787. [PubMed: 15860727]

Lee JH, Lee E, Park J, Kim E, Kim J, Chung J. In vivo p53 function is indispensable for DNA damage-induced apoptotic signaling in Drosophila. FEBS Lett 2003;550:5–10. [PubMed: 12935877]

Lowe SW, Schmitt EM, Smith SW, Osborne BA, Jacks T. p53 is required for radiation-induced apoptosis in mouse thymocytes. Nature 1993;362:847–849. [PubMed: 8479522]

Nolo R, Morrison CM, Tao C, Zhang X, Halder G. The bantam microRNA is a target of the hippo tumor-suppressor pathway. Curr Biol 2006;16:1895–1904. [PubMed: 16949821]

Ollmann M, Young LM, Di Como CJ, Karim F, Belvin M, Robertson S, Whittaker K, Demsky M, Fisher WW, Buchman A, Duyk G, Friedman L, Prives C, Kopczynski C. Drosophila p53 is a structural and functional homolog of the tumor suppressor p53. Cell 2000;101:91–101. [PubMed: 10778859]

Peters M, DeLuca C, Hirao A, Stambolic V, Potter J, Zhou L, Liepa J, Snow B, Arya S, Wong J, Bouchard D, Binari R, Manoukian AS, Mak TW. Chk2 regulates irradiation-induced, p53-mediated apoptosis in Drosophila. Proc Natl Acad Sci U S A 2002;99:11305–11310. [PubMed: 12172011]

Rong YS, Titen SW, Xie HB, Golic MM, Bastiani M, Bandyopadhyay P, Olivera BM, Brodsky M, Rubin GM, Golic KG. Targeted mutagenesis by homologous recombination in D. melanogaster. Genes Dev 2002;16:1568–1581. [PubMed: 12080094]

Ryoo HD, Gorenc T, Steller H. Apoptotic cells can induce compensatory cell proliferation through the JNK and the Wingless signaling pathways. Dev Cell 2004;7:491–501. [PubMed: 15469838]

Schuler M, Green DR. Mechanisms of p53-dependent apoptosis. Biochem Soc Trans 2001;29:684–688. [PubMed: 11709054]

Sogame N, Kim M, Abrams JM. Drosophila p53 preserves genomic stability by regulating cell death. Proc Natl Acad Sci U S A 2003;100:4696–4701. [PubMed: 12672954]

Takai H, Naka K, Okada Y, Watanabe M, Harada N, Saito S, Anderson CW, Appella E, Nakanishi M, Suzuki H, Nagashima K, Sawa H, Ikeda K, Motoyama N. Chk2-deficient mice exhibit radioresistance and defective p53-mediated transcription. Embo J 2002;21:5195–5205. [PubMed: 12356735]

Tang G. siRNA and miRNA: an insight into RISCs. Trends Biochem Sci 2005;30:106–114. [PubMed: 15691656]

Thompson BJ, Cohen SM. The Hippo pathway regulates the bantam microRNA to control cell proliferation and apoptosis in Drosophila. Cell 2006;126:767–774. [PubMed: 16923395]

Wells BS, Yoshida E, Johnston LA. Compensatory proliferation in Drosophila imaginal discs requires Dronc-dependent p53 activity. Curr Biol 2006;16:1606–1615. [PubMed: 16920621]

Wichmann A, Jaklevic B, Su TT. Ionizing radiation induces caspase-dependent but Chk2- and p53-independent cell death in Drosophila melanogaster. Proc Natl Acad Sci U S A 2006;103:9952–9957. [PubMed: 16785441]

Zhou X, Wang G, Zhang W. UV-B responsive microRNA genes in Arabidopsis thaliana. Mol Syst Biol 2007;3:103. [PubMed: 17437028]

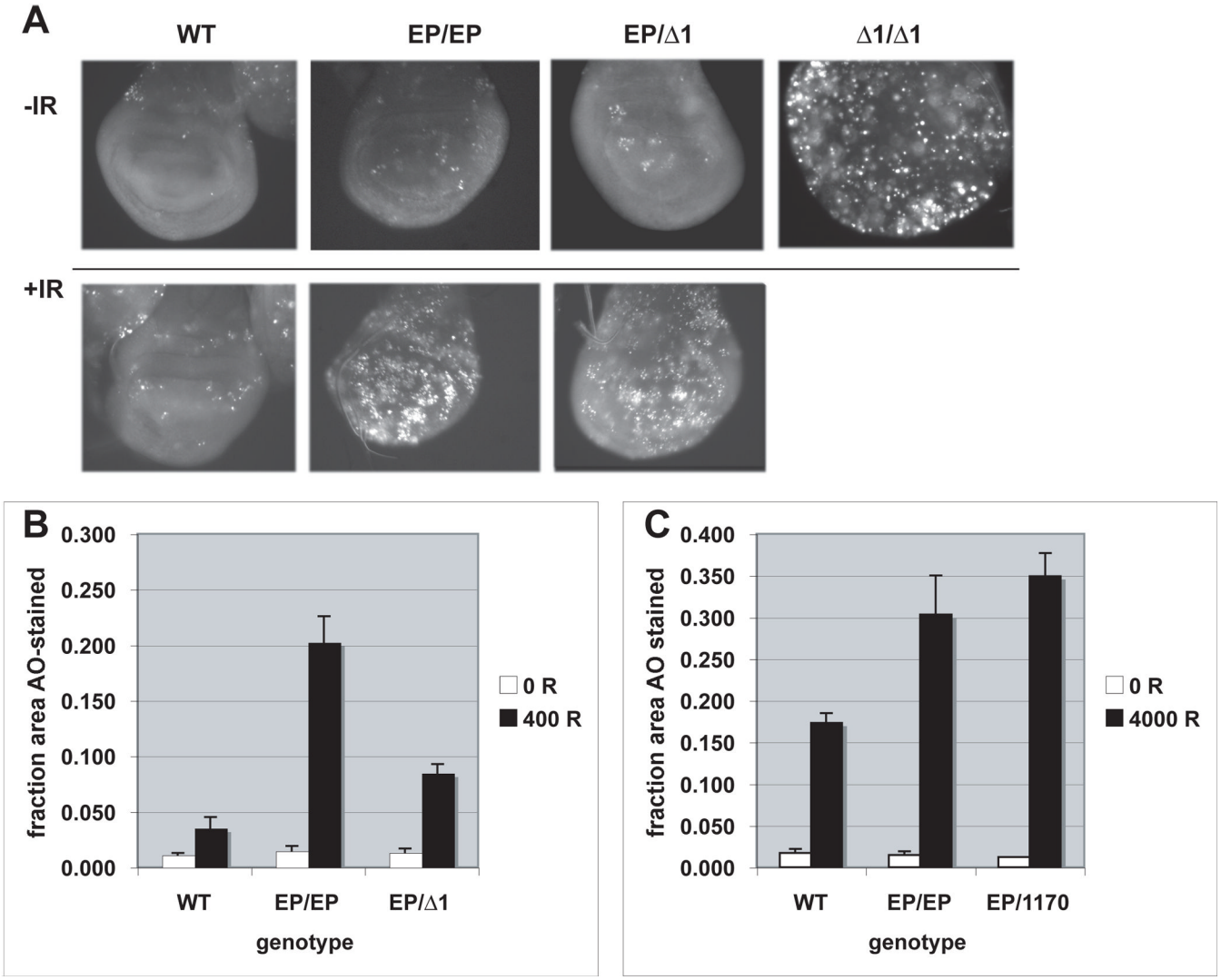

FIGURE 1. Apoptosis after irradiation in *ban* mutants

(A) Wing imaginal discs were dissected from larvae 3.5–4 hr after irradiation with 0 (−IR) or 400 R (+IR) of X-rays and stained with Acridine Orange. (B) The fractional area of each disc that was stained with AO was quantified using NIH Image-J software. The data are from 12 (WT−IR), 25 (WT+IR), 5 (EP/EP−IR), 15 (EP/EP+IR), 9 (EP/Δ1−IR) and 7 (EP/Δ1+IR) discs in at least three experiments. Error bars = SEM. WT = Sevelin wild type; EP/EP = ban^{EP3362} homozygotes. Δ1/EP= ban^{EP3362}/ $ban^{\Delta 1}$ hemizygotes. Δ1/Δ1= $ban^{\Delta 1}$ homozygotes, which show apoptosis in imaginal discs even in the absence of irradiation; discs from these animals flatten readily under a cover slip in these live samples, thus appearing larger than others. The data are from 5–25 discs per genotype per condition in at least 3 independent experiments. The differences between −IR and +IR samples are statistically significant ($p<0.05$) for all three genotypes shown.

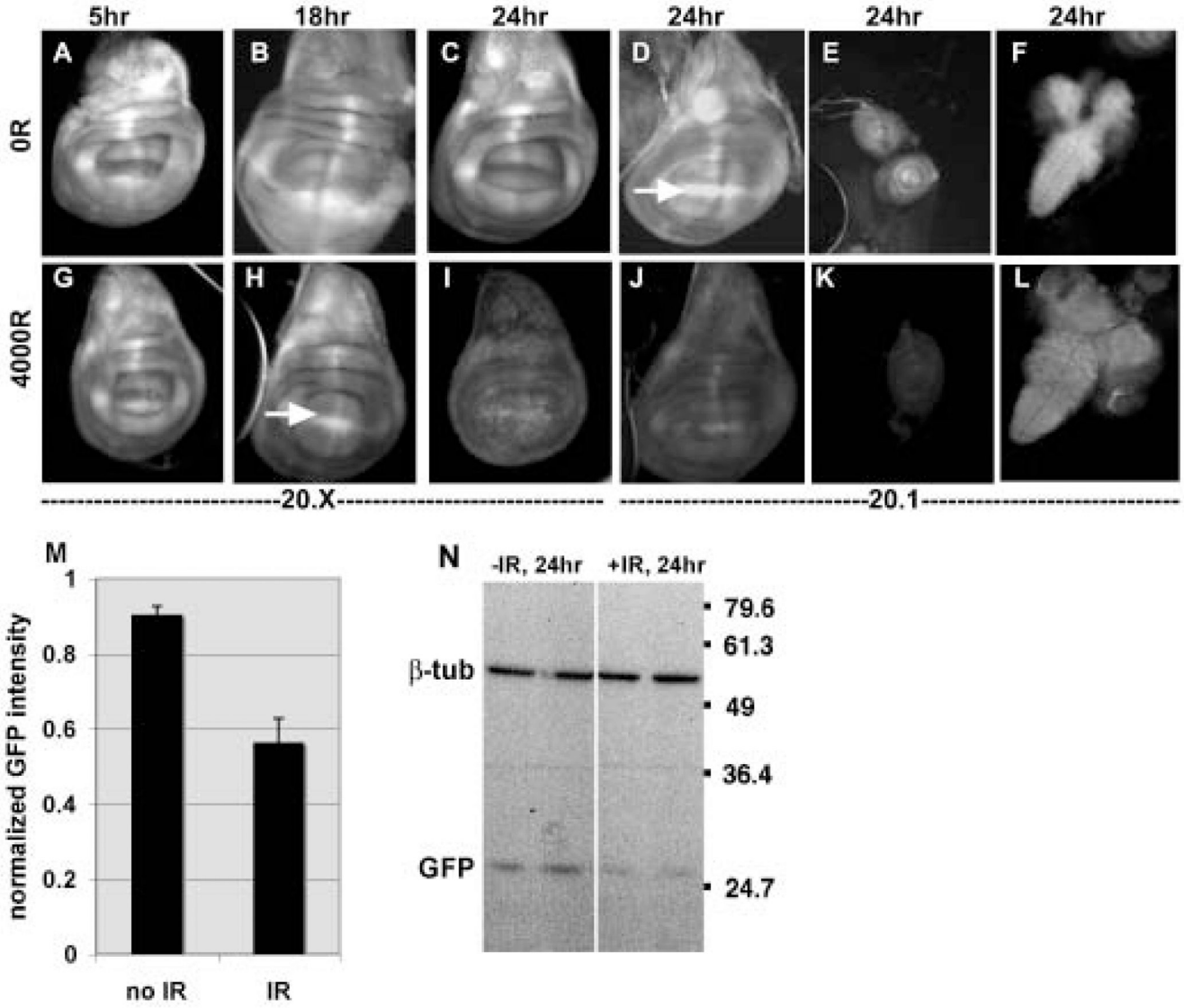

FIGURE 2. *bantam* sensor expression is reduced in irradiated imaginal discs

Wing imaginal discs (A–D and G–J), leg imaginal discs (e and K) and the CNS (brains and Ventral Nerve Cord; F and L) from 3rd instar larvae were imaged for EGFP fluorescence at 5, 18 or 24 hr after exposure to 0 or 4000R of X-rays. Each irradiated tissue was imaged, and the images processed identically as for un-irradiated counterparts to allow direct comparison (e.g. unirradiated wing discs to irradiated wing discs; unirradiated leg discs to irradiated leg discs). '20.1' and '20.X' refer to different insertion lines that carry the Tub-EGFP sensor (Brennecke et al., 2003). Note that local enrichment of *ban* sensor expression, for example at the D/V boundary (Brennecke et al., 2003), is visible in some discs (arrows in D and H) but not others because of the focal plane shown.

(M) Mean GFP fluorescence from larval wing imaginal discs 24 hr after exposure to 0R (no IR) or 4000–5000R of X-rays (IR) were normalized and averaged as explained in Methods. The data are from 15 (no IR) and 15 (IR) discs in 4 different experiments of both 20.X and 20.1 insertion lines. Because of sample thickness, images from more than one focal plane were considered in determination of mean intensity. The decrease in GFP signal in irradiated discs is significant ($p=0.0017$). Error bars=1 SEM.

(N) The level of EGFP was analyzed by Western blotting of extracts from CNS and imaginal discs from larvae 24 hr after exposure to 0R (−IR) or 4000R (+IR) of X-rays. Duplicate samples are blotted for each condition. Extracts from equivalent number of larvae were loaded and β-tubulin serves as a loading control.

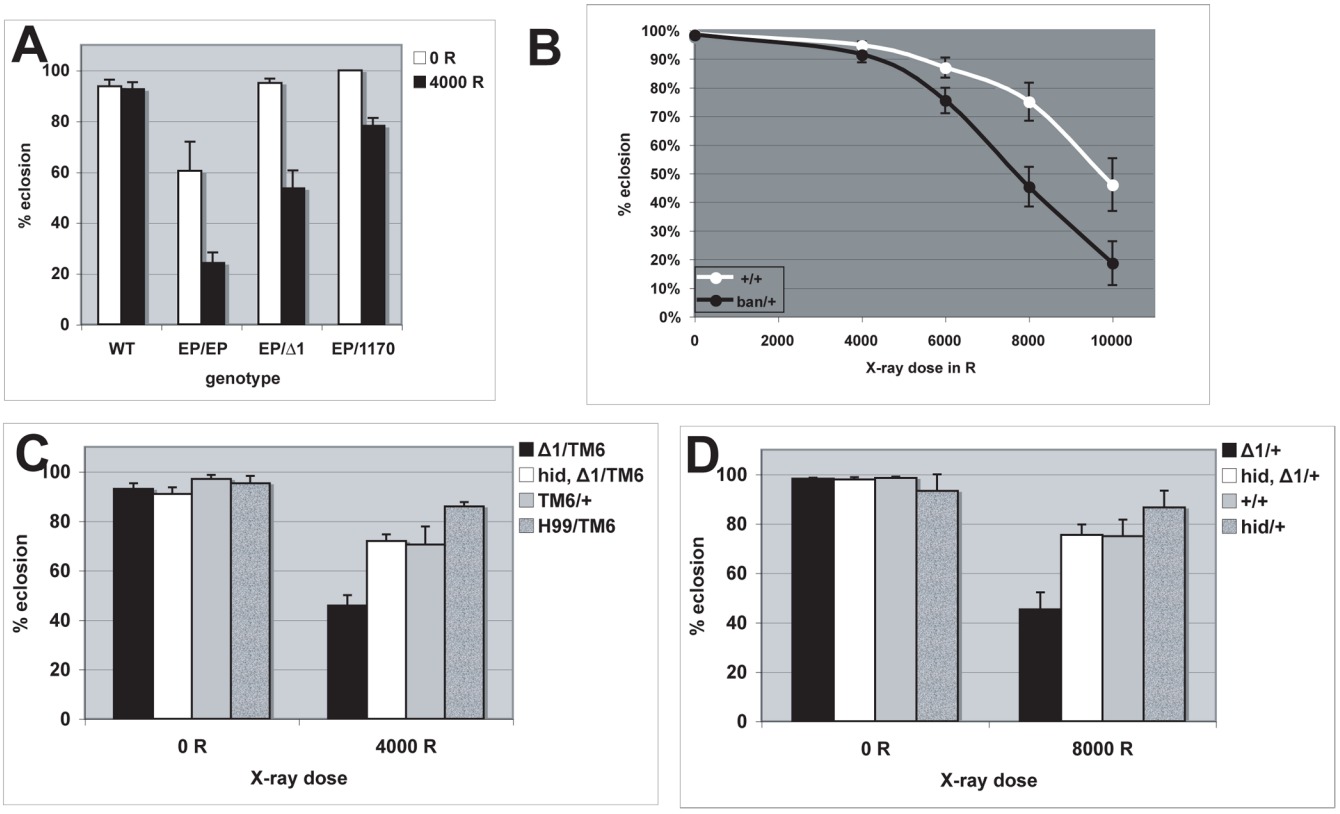

FIGURE 3. Radiation sensitivity of *ban* mutants and rescue by a mutation in *hid*

Larvae were irradiated at 96±4 hr after egg deposition with doses of X-rays shown. All irradiated larvae formed pupae. Percent of pupae that eclosed into adults were quantified 10 days after irradiation. The data are from at least 3 separate experiments for each treatment. The total number of pupae counted ranged from 259 to 4873 per sample. Homozygous or hemizygous *ban* mutants were distinguished from heterozygous siblings by the lack of the Tubby (TB) marker on the balancer chromosome.

(A) *ban* mutants show significantly decreased eclosion after irradiation ($p<0.001$), where as eclosion of wild type (WT) larvae did not change significantly ($p=0.307$). EP/EP = ban^{EP3362} homozygotes. Δ1/EP= ban^{EP3362}/ $ban^{\Delta 1}$ hemizygotes.

(B) $ban^{\Delta 1}$ heterozygotes (Δ1/TM6) show significantly reduced eclosion after irradiation ($p<0.001$). *hid* mutation rescued the survival such that *hid*, $ban^{\Delta 1}$ heterozygotes (hid,Δ1/TM6) show comparable eclosion as balancer controls (TM6/+). Heterozygotes of a chromosomal deletion Df(3)H99 that removes Hid (H99/TM6) show that heterozygocity for *hid* alone has little effect on radiation survival. Student t-tests were used to generate p-values. Error bar= one standard deviation.

The data are from at least 3 independent experiments per genotype per condition.

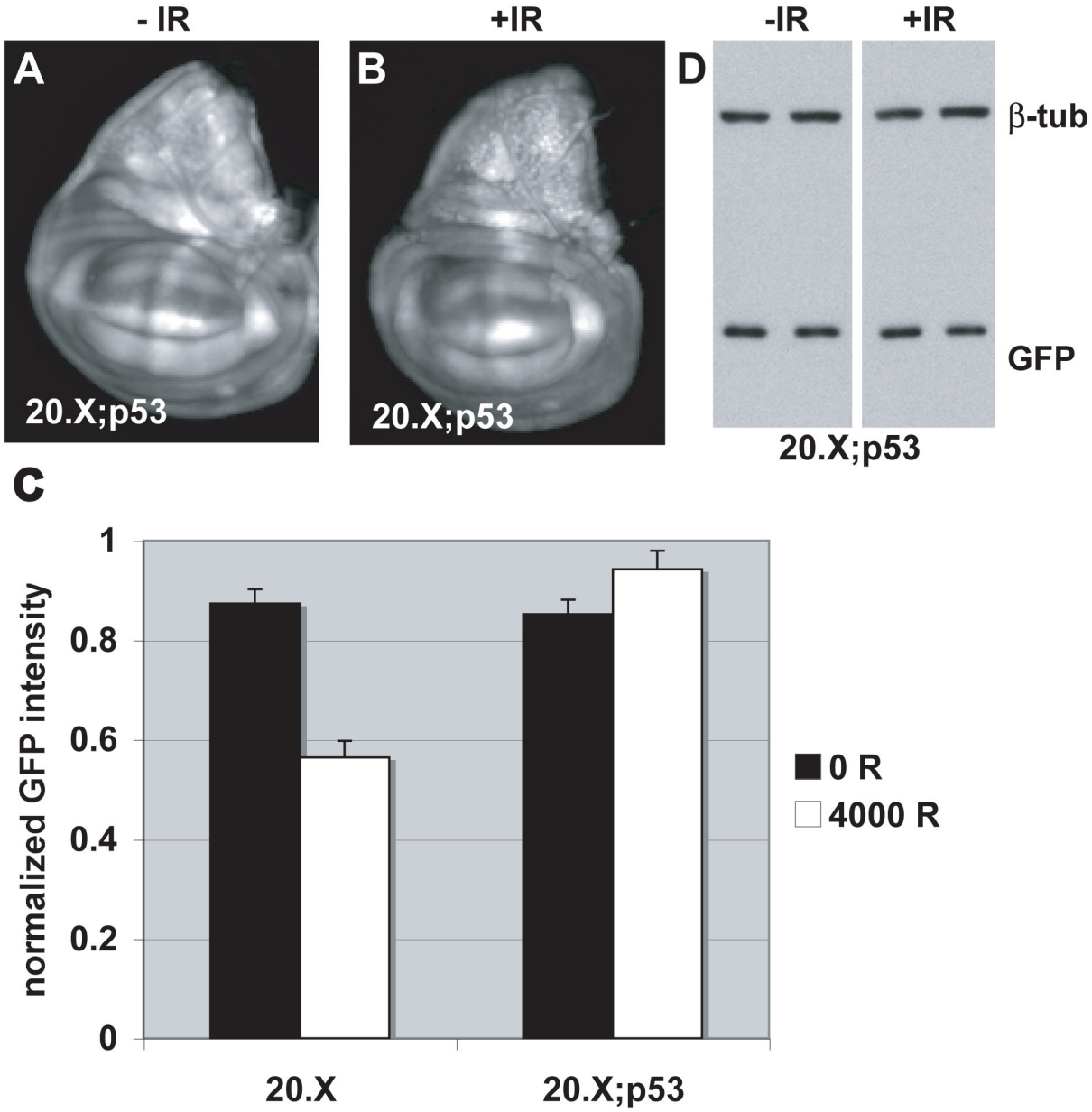

FIGURE 4. ***ban*** **sensor expression remains unchanged after irradiation in p53 mutants**

(A, B) Wing imaginal discs from control (A) and irradiated larvae (B) are imaged for EGFP fluorescence 24 hr after irradiation with 4000 R of X-rays. Larvae were homozygous for $p53^{5A\text{-}1\text{-}4}$ and the 20.X *ban* sensor.

(C) Mean GFP fluoresence intensity for wing imaginal discs analyzed as described in Fig. 2M, at 24 hr after irradiation with doses shown. The decrease in GFP signal in irradiated discs is significant for the controls (20.X) (p=0.00004) but not for p53 mutants (20.X; p53) (p=0.14). The data are from 14 (20.X, no IR) and 10 (20.X, IR), 14 (20.X; p53, no IR) and 12 (20.X; p53, IR) discs in 2 different experiments. Error bars=1 SEM. 20.X = homozygous ban sensor. 20.X; p53 = the same in homozygous $p53^{5A\text{-}1\text{-}4}$ background.

(D) The level of EGFP in the above experiment was analyzed by Western blotting of extracts from larval CNS and imaginal discs from homozygous $p53^{5A\text{-}1\text{-}4}$ larvae that carry the 20.X

ban sensor. No change in GFP was detected. Duplicate samples were blotted for each condition. Extracts from equivalent number of larvae were loaded and β-tubulin serves as a loading control.

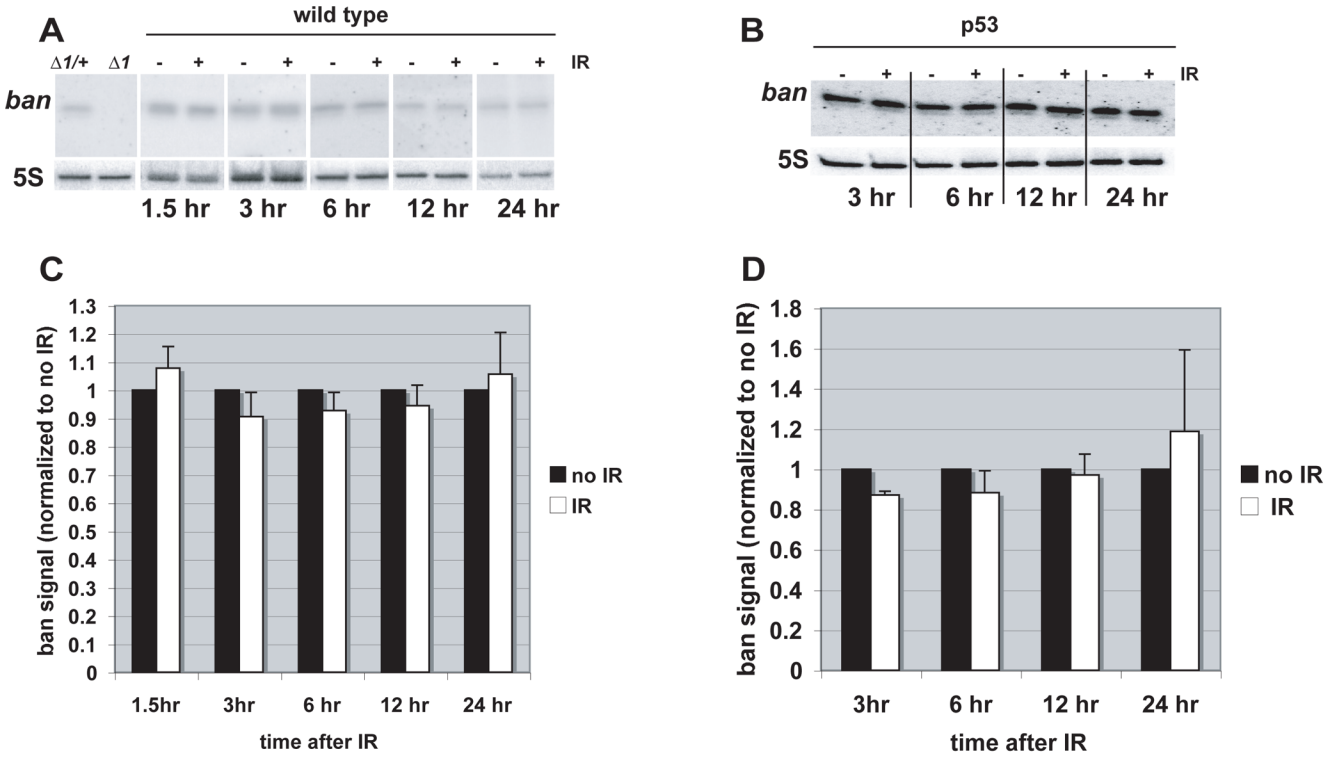

FIGURE 5. *ban* miRNA levels do not change after irradiation

(A) Total RNA extracted from whole larvae was Northern blotted for mature *ban*. *ban* signal was detected in extracts from $ban^{\Delta 1}$ heterozygotes (*Δ1*/+) but not homozygotes (*Δ1*), indicating the specificity of the probe. Where indicated, larvae (wild type) had been exposed to 0 (−) or 4000 R (+) of X-rays and allowed to rest for indicated times before RNA extraction. 5S RNA serves as a loading control. (B) Quantification of Northern blots shows no significant change in *ban* miRNA levels after irradiation. For each time point, the signals were normalized to that of no IR controls. Error bars = SEM. The data are from 3–6 independent samples per time point per condition.

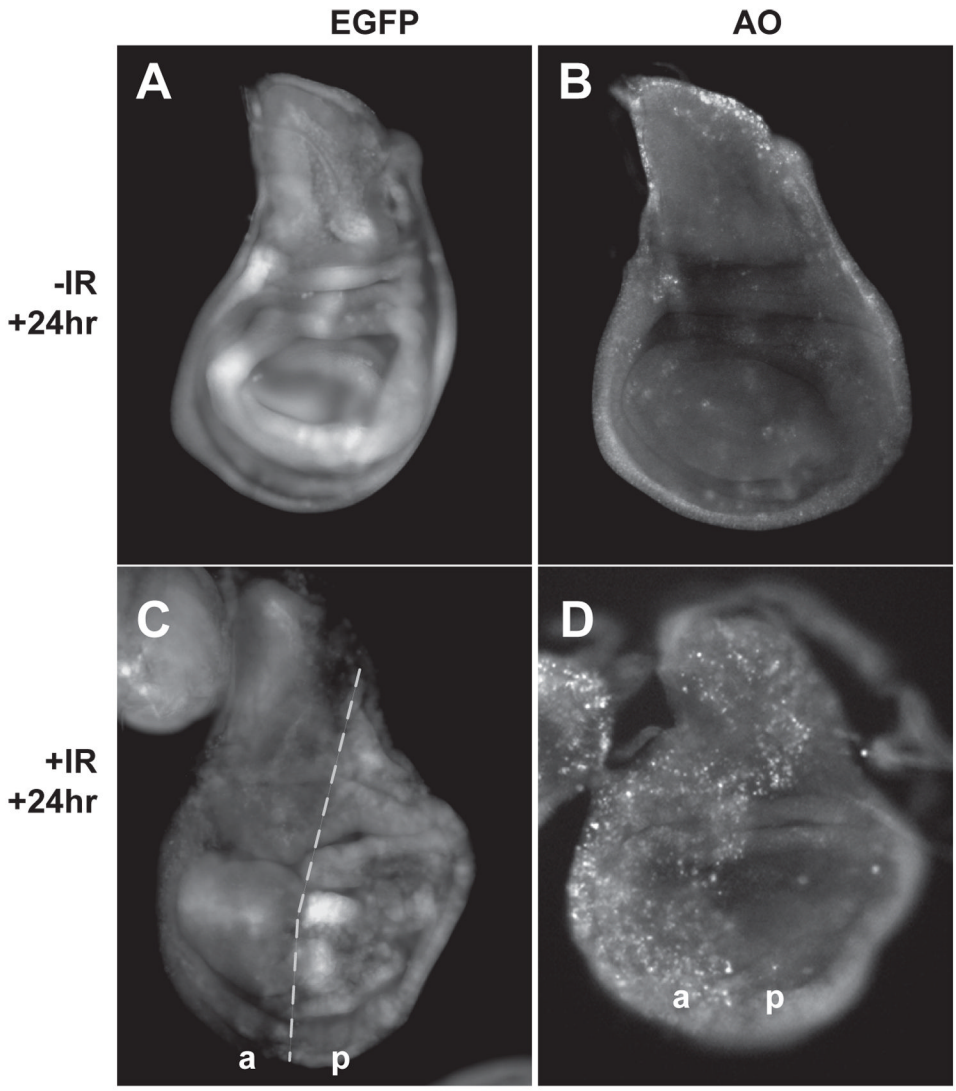

FIGURE 6. Blocking cell death reduced changes in *ban* sensor after irradiation

Wing imaginal discs from control (A,B) and irradiated larvae (C,D) are imaged for EGFP fluorescence from the *ban* sensor (A,C) or Acridine Orange staining (B,D) 24 hr after irradiation with 0 or 4000 R of X-rays. Larvae were products of a cross between 20.X;hh-GAL4 and 20.X; UAS-p35 homozygous flies. Hh-GAL4>UAS-p35 inhibits IR-induced cell death in the posterior compartment (D). The IR-induced decrease in *ban* sensor expression was seen in the anterior compartment (a) but not in the posterior compartment (p). Similar differences in the sensor expression from (a) and (p) compartments were observed in 13 of 13 discs in 2 different experiments. Note that EGFP and AO images show slight differences in morphology and orientation. This is because the discs were first imaged for EGFP, recovered from microscope slides, stained with AO, remounted on slides before being imaged for AO.

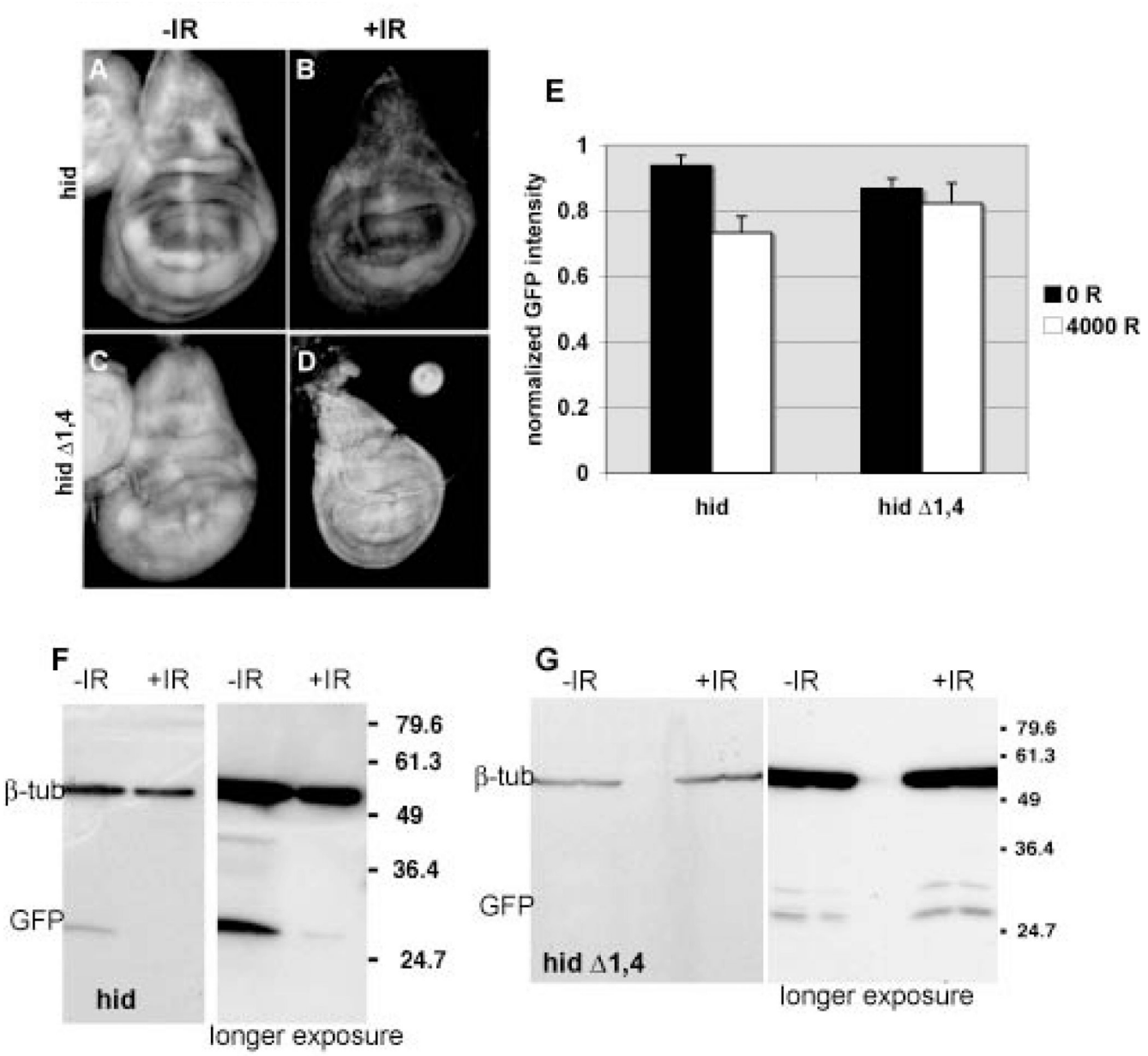

FIGURE 7. *hid-3'UTR* sensor expression is reduced in irradiated imaginal discs

Wing imaginal discs from control (A,C) and irradiated larvae (B,D) are imaged for EGFP fluorescence 24 hr after irradiation with 4000 R of X-rays. Larvae carry the *hid-3'UTR* sensor (A,B; 'hid') or the *hid-3'UTR* sensor lacking the two best matching *ban* target sites (C,D; 'hid Δ1,4') in homozygous state.

(E) Mean GFP fluoresence intensity for wing imaginal discs analyzed as described in Fig. 2M, at 24 hr after irradiation with doses shown. The decrease in GFP signal in irradiated discs is significant for the *hid-3'UTR* sensor (hid) (p=0.0017) but not for the *hid-3'UTR* sensor lacking two best matching *ban* target sites (hid Δ1,4) (p=0.82). The data are from 7 (hid, no IR) and 10 (hid, IR), 9 (hid Δ1,4, no IR) and 7 (hid Δ1,4, IR) discs in 3 different experiments. Error bars=1.

(D) The level of EGFP in the above experiment was analyzed by Western blotting of extracts from larval CNS and imaginal discs. A decrease in GFP was detected for the *hid-3'UTR* sensor

(hid) but not for the *hid-3'UTR* sensor lacking two best matching *ban* target sites (hid Δ1,4). Duplicate samples were blotted for each condition. The expression of GFP from 'hid Δ1,4' is low; the short exposure of the gel is shown for comparisons of the β-tubulin signal and the long exposure is shown for comparison of the GFP signal. Extracts from equivalent number of larvae were loaded and β-tubulin serves as a loading control.